Supplementary Table S1: Primer sequences used in this study

Gene	Forward (5'-3')	Reverse (5'-3')
TBX3-1	ACACTGGAAATGGCCGAAGA	GCTTGTTCACTGGAGGACTCA
TBX3-2	TCTGAAACCGACGTTCAGGAG	TGCACTTCAAAGGGAGGAGG
TBX4-1	GCATGAACCCCAAGACCAAG	CCCTGCCACCATCCATTTGT
TBX4-2	AGAACAATGCTTTCGGCTCCA	TCACGGGGTATTCTTTGCTCT
TBX5	CAGTTACAAAGTGAAGGTGACG	TGCGAATTTGTATCTGTGATCG
TBX6	CTATGGGAGCGGAGACACAC	CTCCTGGTGGGAAGGTGACT
TBX15	CCAACTTTTCATCTGGCCCC	CTCTGAAGCCTGTTGTAGCCA
BACH1	AAATGAATGCCTGGGAGGAGT	AATTGTGGGGGAAAGGAGTCA
BACH2	ATGGATTGCCAGAGCCTTCTCAT	TGCCGTTCACACCATGTAATTT
MYC	CTCCTACGTTGCGGTCACAC	GGTTCACCATGTCTCCTCCC
SPATS1	TTTAGCAGCAACATCCACACCTACC	AGCACTTGTCCACCGTCCTCTC
HOXD3	AGAGAGCTGCGAGGACAAGA	ACAAGTAGCGGTTGAAGTGGA
ETV1	TCTGGATACTGGCTACTGGCTACTG	AGGCTGGAGACAACAATGTGGAAG
CDH26	CTTAGGTGGCTGTTCTGGCGATG	GTGACACTGGTGACAATGAGGATGG
DUXA	GCATGGCCGAAGACACCTAT	TGTGTAACTGAGAGGCGCTG
SLC1A4	TGAGGCTTACCTCTCGGCA	CTGGACATGGATCAAGCCGAA
SLC1A5	GGTTACTCCTCAAAACCCCCA	GTGACCTGCTCCCTGAGACA
SLC38A1	GCATTTGTTTGCCACCCGTC	CGGACTGCACGTTGTCATAG
SLC38A2	AGATTTCAGTTGGTGGCGTC	TAACAGGAAGAACAAAGCCCCA
GLS	GTCCCGATTTGTGGGGTGT	GGACTGAAGACAGAAGGGAACT
GLUD1	TCAGCTATGGCCGTTTGACC	GCCGTGGGTACAATGGGAA
ASNS	TGTTGGATGGTGTGTTTGCATTT	GTCGCGGAGTGCTTCAATGT
PHGDH	GAACACCCCCAATGGGAACA	GCCTGGGGAATCTGCCTG
β-ACTIN	CTCCATCCTGGCCTCGCTGT	GCTGTCACCTTCACCGTTCC

Supplementary Table S2: Relationships between SLC1A5 expression and the clinicopathological characteristics of NSCLC patients.

Variables	SLC1A5 staining			Total	*P value*
	High (%)	Middle (%)	Low (%)		
Gender					
Female	30 (33.7)	51 (57.3)	8 (8.9)	89	0.7565
Male	39 (30.0)	81 (62.3)	10 (7.7)	130	
Age					
≤50	19 (32.8)	31 (53.4)	8 (13.8)	58	0.1627
>50	50 (31.1)	101 (62.7)	10 (6.2)	161	
Pathologic type					
LUAD	34 (25.6)	85 (63.9)	14 (10.5)	133	0.0345
LUSC	35 (40.7)	47 (54.6)	4 (4.7)	86	
Lymph node metastasis					
Negative	38 (27.5)	83 (60.1)	17 (12.3)	138	0.0087
Positive	31 (38.3)	49 (60.5)	1 (1.2)	81	
Distant metastasis					
M0	64 (31.1)	124 (60.2)	18 (8.7)	206	0.5087
M1	5 (38.5)	8 (61.5)	0 (0.0)	13	
Tumor stage					
I~II	19 (21.6)	55 (62.5)	14 (15.9)	88	0.0005
III~IV	50 (38.2)	77 (58.8)	4 (3.1)	131	
EGFR status					
Negative	15 (36.5)	24 (58.5)	2 (4.9)	41	0.6303
Positive	7 (25.9)	18 (66.7)	2 (7.4)	27	

Supplementary Table S3: The relationship between the level of SLC1A5 and tumor stage and lymphatic metastasis in patients with LUAD and LUSC.

Variables	LUAD			*P value*	LUSC			*P value*
	High (%)	Middle (%)	Low (%)		High (%)	Middle (%)	Low (%)	
Lymph node metastasis								
Negative	21 (25.3)	48 (57.8)	14 (16.9)	0.0078	17 (30.9)	35 (63.6)	3 (5.5)	0.0434
Positive	13 (26.0)	37 (74.0)	0 (0.0)		18 (58.1)	12 (38.7)	1 (3.2)	
Tumor stage								
I~II	11 (22.4)	26 (53.1)	12 (24.5)	0.0003	8 (20.5)	29 (74.4)	2 (5.1)	0.0026
III~IV	23 (27.4)	59 (70.2)	2 (2.4)		27 (57.4)	18 (38.3)	2 (4.3)	

Supplementary Table S4: Anti-body and reagents used in this study

REAGENT or RESOURCE	SOURCE	IDENTIFIER
Antibodies		
Rabbit Polyclonal anti-SLC1A4	Proteintech	Cat#13067-2-AP
Rabbit Polyclonal anti-SLC1A5	Proteintech	Cat#20350-1-AP
Rabbit polyclonal anti-HK2	Proteintech	Cat#22029-1-AP
Rabbit polyclonal anti-PFKFB3	Proteintech	Cat#13763-1-AP
Rabbit polyclonal anti-MCT1	Proteintech	Cat#20139-1-AP
Rabbit polyclonal anti-GPI	Proteintech	Cat#15171-1-AP
Rabbit polyclonal anti-HIF1a	Proteintech	Cat#20960-1-AP
Rabbit polyclonal anti-GAPDH	Proteintech	Cat#10494-1-AP
Rabbit Polyclonal anti-C-MYC	Proteintech	Cat#10828-1-AP
Rabbit Polyclonal anti-BACH1	Proteintech	Cat#14018-1-AP
Rabbit Polyclonal anti-Alpha Tubulin	Proteintech	Cat#14018-1-AP
Rabbit Polyclonal anti-TBX4	ABclonal	Cat#A10691
Rabbit Polyclonal anti-TBX15	ABclonal	Cat#A10481
Chemicals, Peptides, and Recombinant Protein		
Seahorse XF 1.0 M glucose solution	Aligent	Cat#103577-100
Seahorse XF 100 mM pyruvate solution	Aligent	Cat#103578-100
Seahorse XF 200 mM glutamine solution	Aligent	Cat#103579-100
JQ1	MedChemExpress	Cat#HY-13030
Critical Commercial Assays		
Cell-Light EdU Apollo567 In Vitro Kit	Ribobio	Cat#C10310-1
Meilun Reactive Oxygen Species Assay Kit	Meilunbio	Cat#MA0219-1
Image-iT Hypoxia Reagents	Invitrogen	Cat#I14834
Annexin V-FITC Apoptosis Detection Kit	KeyGEN BioTECH	Cat#KGA108
Human Gln ELISA Kit	RENJIEBIO	Cat#RJ12495
Human GSH ELISA Kit	RENJIEBIO	Cat#RJ12496
Seahorse XF Cell Mito Stress Test Kit	Aligent	Cat#103015-100
Seahorse XF Glycolysis Stress Test Kit	Aligent	Cat#103020-100
UltraSYBR One Step RT-qPCR Kit	CWBIO	Cat#CW0659
HiScript Q RT SuperMix for qPCR	Vazyme	Cat#R123-01
ChIP Assay Kit	Beyotime	Cat#P2078

Supplemental Figures

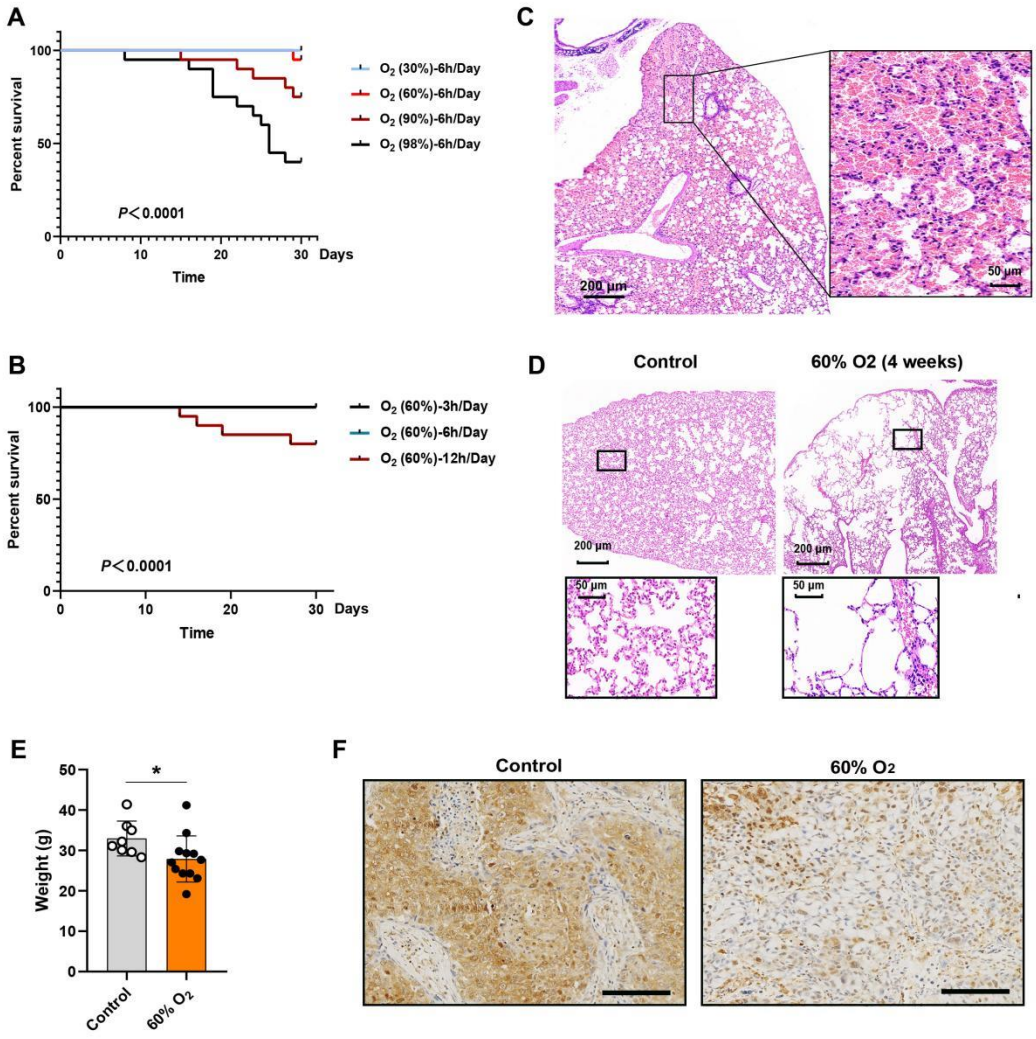

Figure S1. The anti-tumor activity and side effects of IH treatment.

(A, B) Oxygen concentration exceeding 90% or breathing of 60% oxygen for 12 h/Day result in death of tumor-free mice, log-rank test.

(C) Representative H&E staining of lungs with 98% O_2 treatment, bar (left)=200 μm, bar (right)=50 μm.

(D) Representative H&E staining of lungs with 60% O_2 (12 h/Day) treatment, bar (up)=200 μm, bar (down)= 50 μm.

(E) Quantitative analysis of body weight of mice treated with IH treatment (n=12) and the controls (n=8), two-tailed Student's t-test.

(F) Representative images of HMGA2-stained lung sections, bar=100 μm.

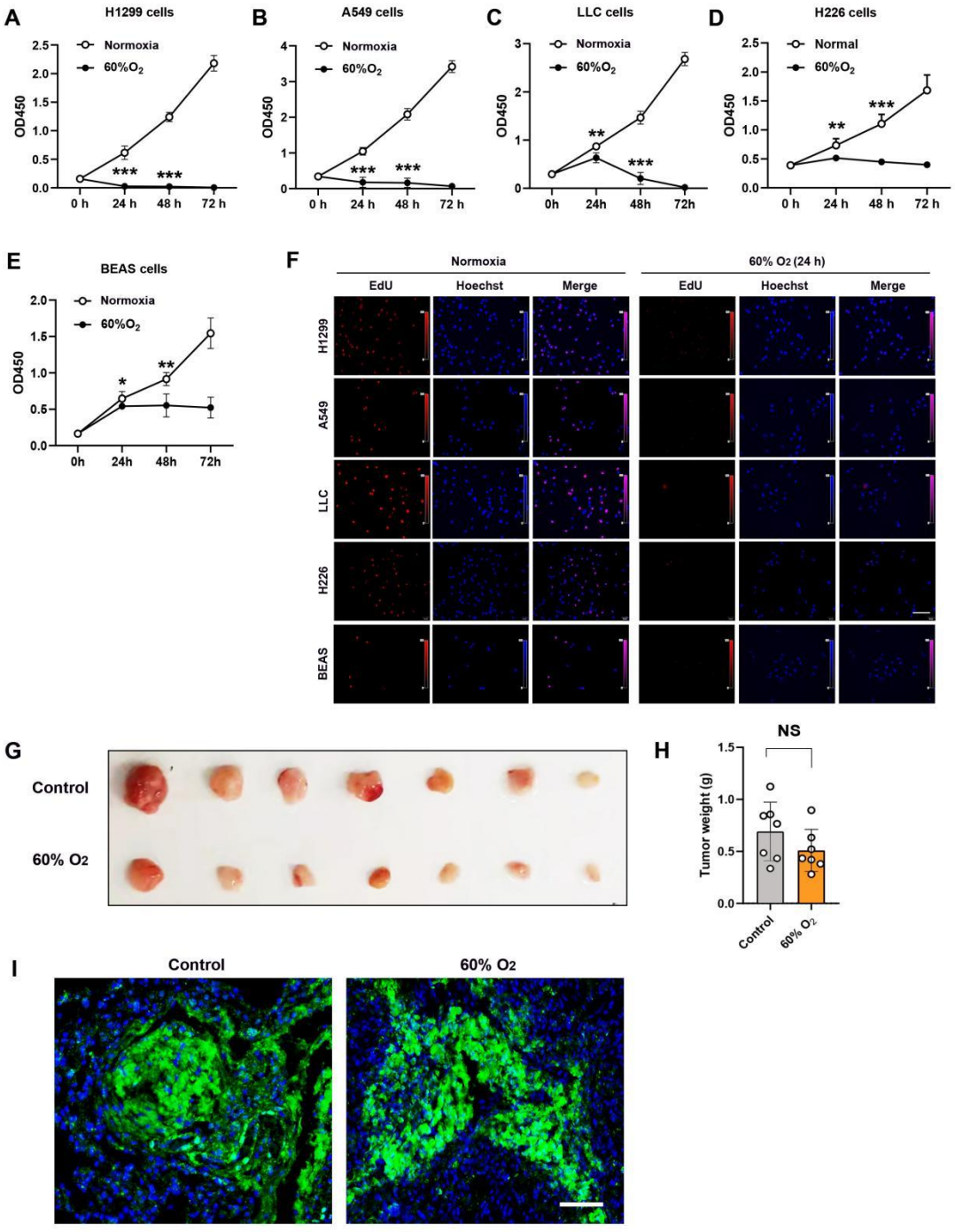

Figure S2. The effect of hyperoxia treatment on the proliferation of BEAS-2b cells and lung cancer cell lines.

(A-E) CCK-8 assay analysis of cell proliferation in H1299, A549, LLC, H226 and BEAS-2b cells (n=5). *$P<0.05$, **$P<0.01$, ***$P<0.001$ vs the normoxia group, two-tailed Student's t-test.

(F) Representative images of EdU and hoechst staining in H1299, A549, LLC, H226 and BEAS-2b cells with 60%O_2 (24 h) treatment, bar=50 μm.

(G, H) IH treatment has no significant effect on the growth of xenograft tumors (n=7), NS, $P > 0.05$ vs the control group, two-tailed Student's t-test.

(I) Image-iT green hypoxia reagent is used to detect hypoxia area in xenograft tumors, bar=100 μm.

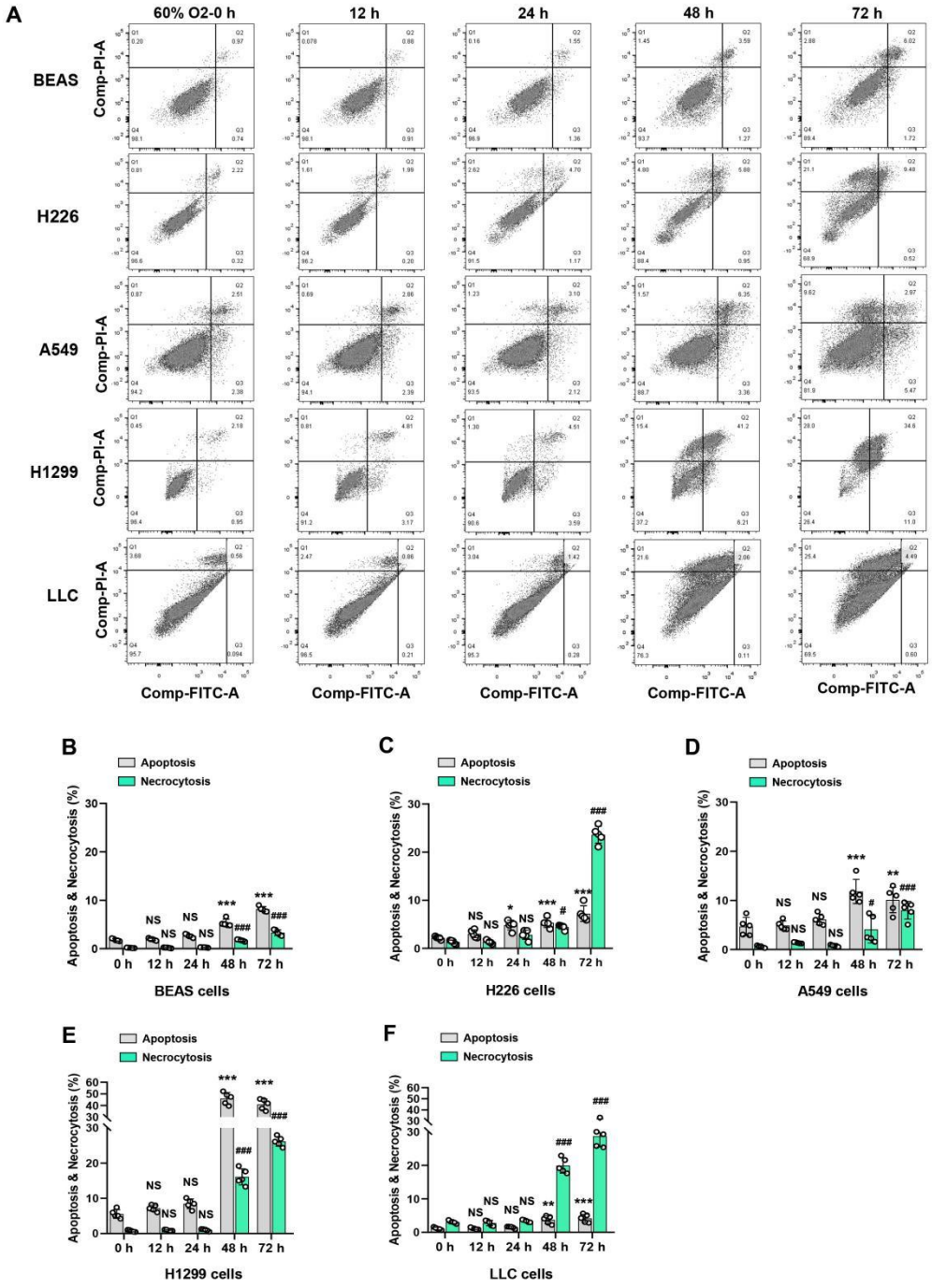

Figure S3. The effects of hyperoxia on cell apoptosis and necrocytosis.

(A-F) Flow cytometric analysis of cells apoptosis and necrocytosis in BEAS-2b, H1299, A549, H226 and LLC cells (n=5). $^{*}P<0.05$, $^{**}P<0.01$, $^{***}P<0.001$, $^{\#}P<0.05$, $^{\#\#\#}P<0.001$, NS, $P>0.05$ vs the 60% O_2 (0 h) group, respectively, one-way ANOVA followed by the Tukey's post hoc test.

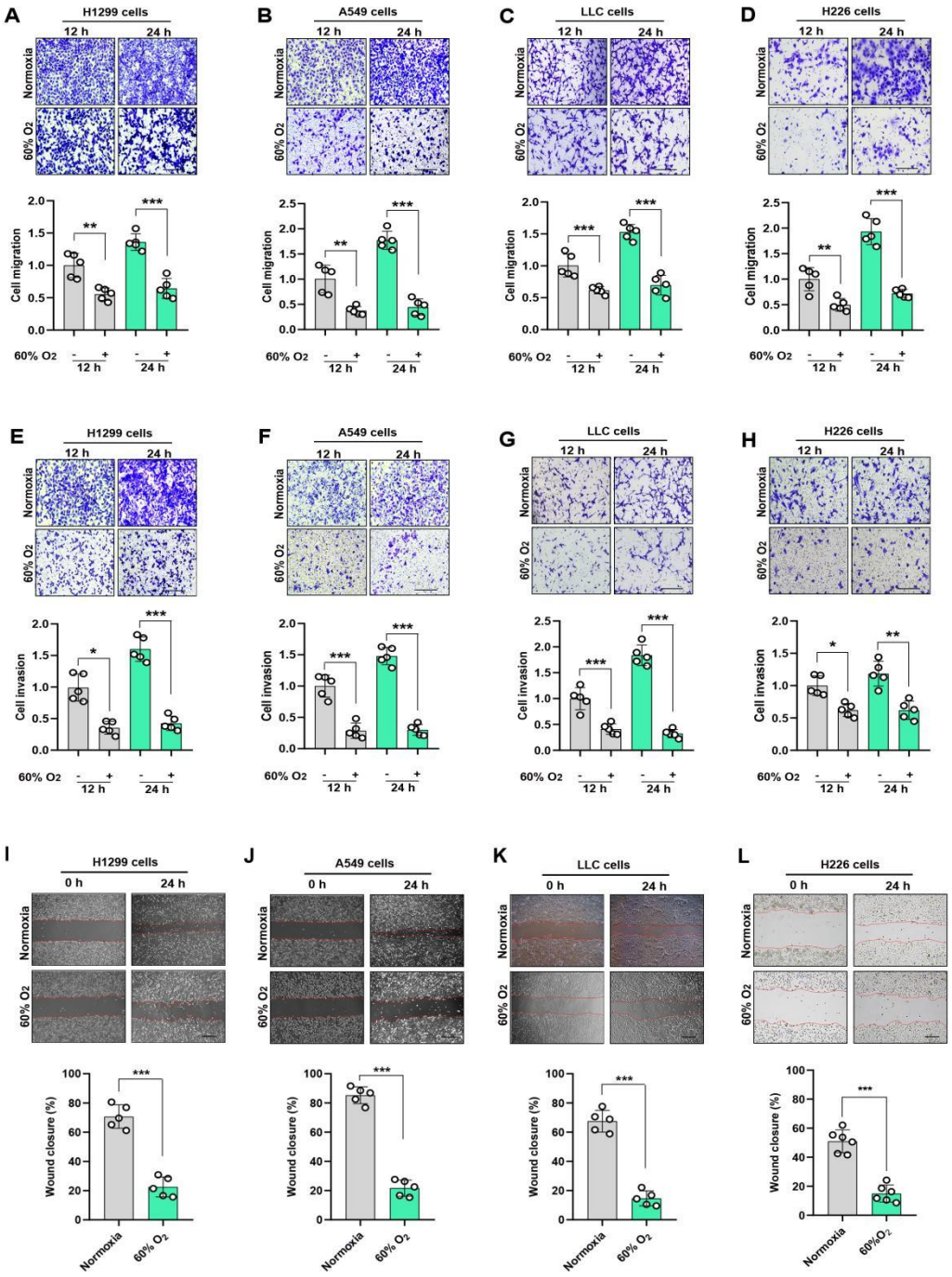

Figure S4. The effects of hyperoxia on cell migration and invasion.

(A-D) Hyperoxia treatment (60% O_2) suppress cell migration in H1299, A549, H226 and LLC cells, bar=50 μm.

(E-H) Hyperoxia treatment (60% O_2) suppress cell invasion in H1299, A549, H226 and LLC cells, bar=50 μm.

(I-L) The wound healing assay was further performed to determine the effect of 60% O_2

(24 h) on the migration of H1299, A549, H226 and LLC cells (n=5), bar=100 μm. *$P<0.05$, **$P<0.01$, ***$P<0.001$ vs the indicated group, two-tailed Student's t-test.

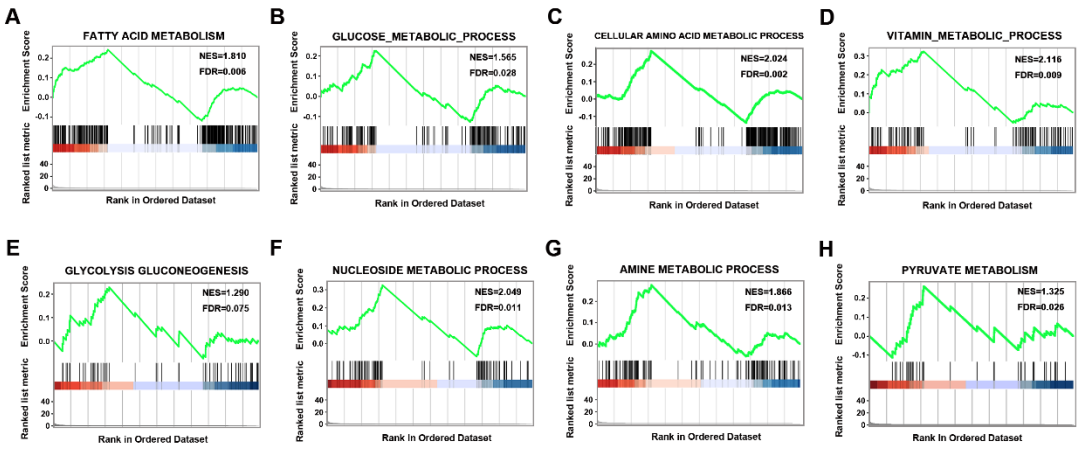

Figure S5. GSEA analysis show significant changes in metabolic pathways in hyperoxia treated H1299 cells.

(A-H) Gene set enrichment analysis of significant differentially expressed mRNA with normalized enrichment score (NES) and false-discovery rate (FDR) Q value.

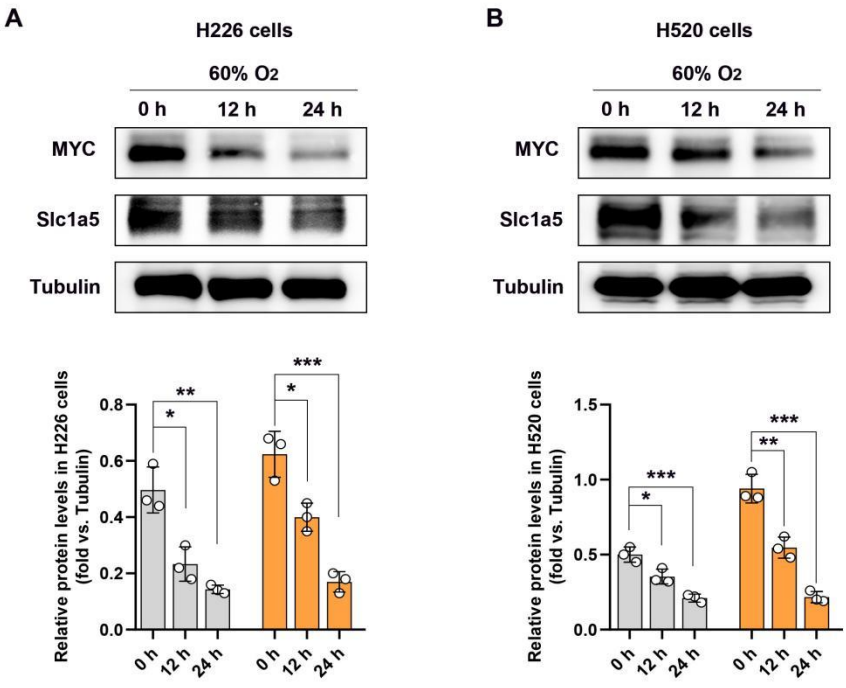

Figure S6. The effects of hyperoxia on the expression levels of MYC and SLC1A5 in LUSC cell lines.

(A) Western blot analysis for the expressions of SLC1A5 and MYC in H226 cells (n=3).

(B) Western blot analysis for the expressions of SLC1A5 and MYC in H520 cells (n=3).

*$P<0.05$, **$P<0.01$, ***$P<0.001$ vs the indicated group, one-way ANOVA followed by the Tukey's post hoc test.

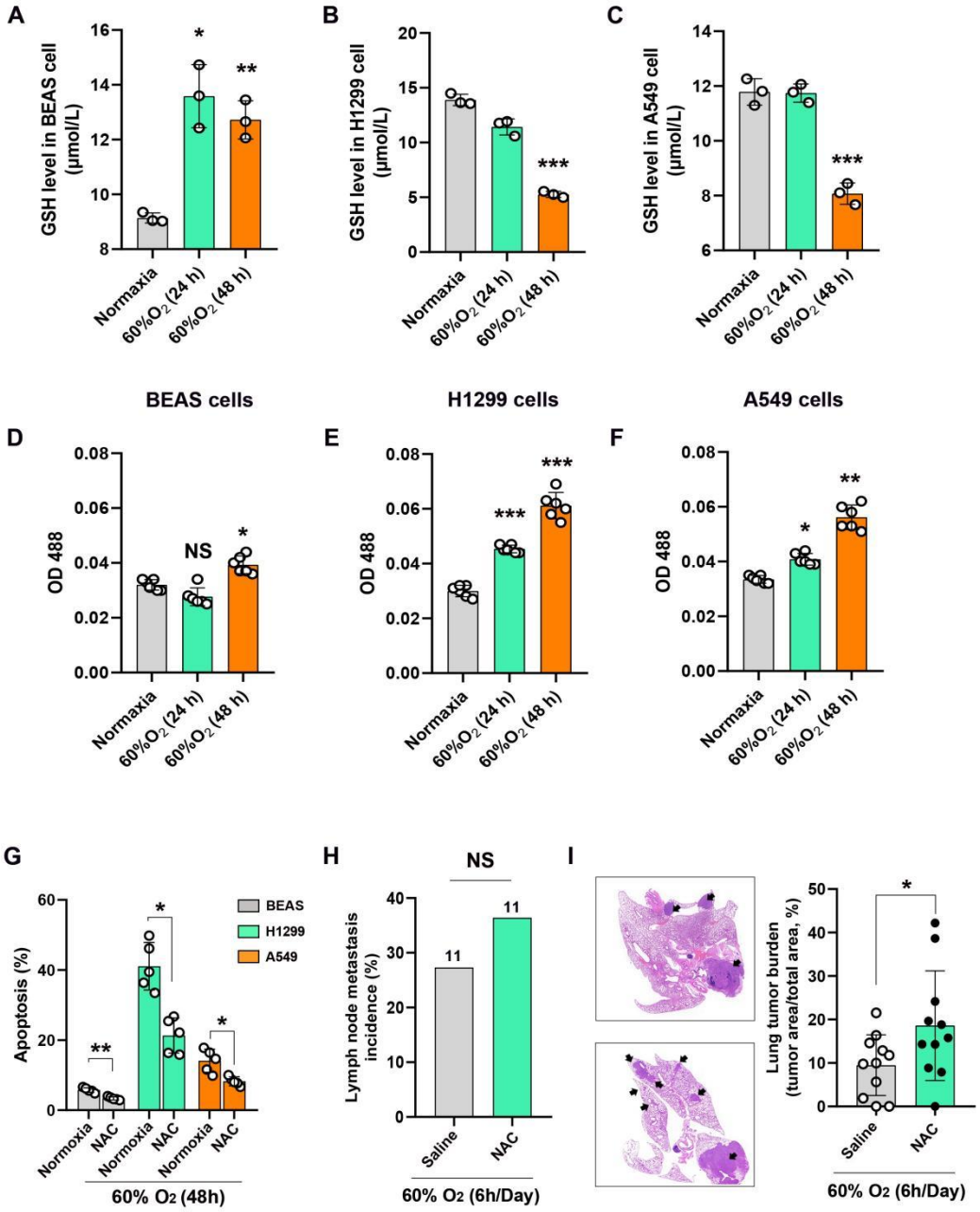

Figure S7. Hyperoxia treatment affects the cellular redox homeostasis of lung cancer cells.

(A-C) Effect of hyperoxia treatment on the levels of glutathione in BEAS-2b, H1299 and A549 cells (n=3).

(D-F) Effect of hyperoxia treatment on the levels of ROS in BEAS-2b, H1299 and A549 cells (n=5).

(G) Flow cytometric analysis of cell apoptosis in BEAS-2b, H1299 and A549 cells incubated with 2 nM NAC (n=5).

(H) Percentage of mice with lymph node metastases ($P>0.05$). NAC is administered in drinking water (1g/L) until the lungs are harvested (n=11), Chi-square test.

(I) Lung tumor burden in mice four weeks after *i.v.* injection of H1299 cells and representative lung section.

*$P<0.05$, **$P<0.01$, ***$P<0.001$, NS, $P>0.05$ vs the normoxia or indicated group, two-tailed Student's t-test.

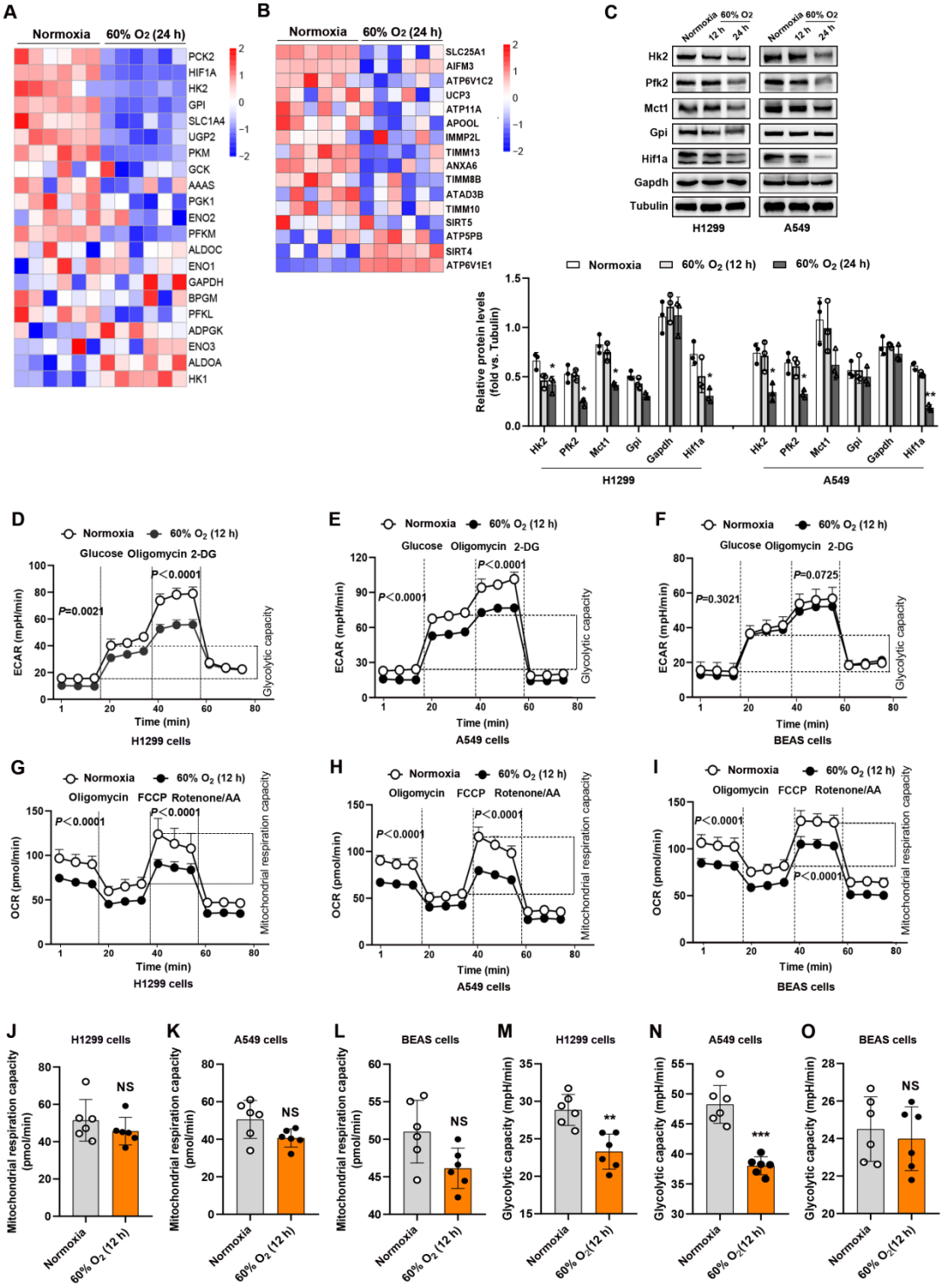

Figure S8. Hyperoxia treatment inhibits glycolysis in lung cancer cell lines.

(A) Heat map depicting changes in the expression of genes involved in “glycolysis” in H1299 cells.

(B) Heat map depicting changes in the expression of genes involved in “mitochondrial

inner membrane” in H1299 cells.

(C) Relative protein expression levels of PFK2, HK2, MCT1, GPI, HIF1α and GAPDH in H1299 and A549 cells treated with 60% O_2 (n=3).

(D-I) Measurements of ECAR and OCR in H1299, A549 and BEAS-2b cells treated with 60% O_2.

(J-O) Effects of hyperoxia treatment on the mitochondrial respiration capacity and glycolytic capacity in H1299, A549 and BEAS-2b cells (n=5).

*$P<0.05$, **$P<0.01$, ***$P<0.001$, NS, $P>0.05$ vs the normoxia group, two-tailed Student’s t-test.

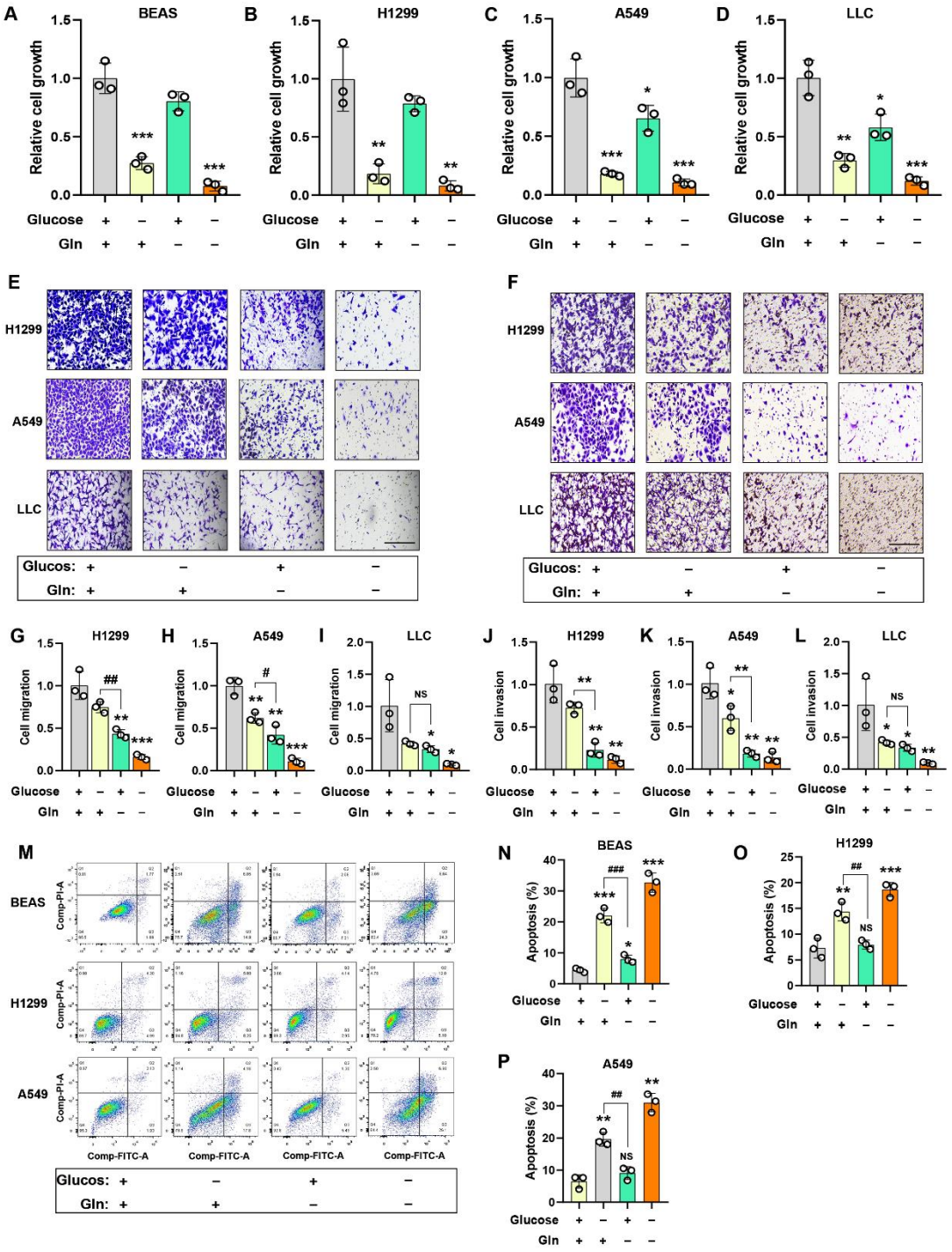

Figure S9. The progression of lung cancer depends on glucose and glutamine catabolism.

(A-D) Effects of glucose deprivation and glutamine deprivation on the proliferation of BEAS-2b, H1299, A549 and LLC cells (n=3). Cells were plated in complete media which was replaced the following day with glucose-free or glutamine-free medium supplemented with 10% fetal bovine serum.

(E-L) Effects of glucose deprivation and glutamine deprivation on the migration and invasion of H1299, A549 and LLC cells (n=3), bar=50 μm.

(M-P) Flow cytometric analysis of cells apoptosis in BEAS-2b, H1299 and A549 cells (n=3).

*$P<0.05$, **$P<0.01$, ***$P<0.001$ vs the control group; $^{\#}P<0.05$, $^{\#\#}P<0.01$, $^{\#\#\#}P<0.001$, NS, $P>0.05$ vs the indicated group, one-way ANOVA followed by the Tukey's post hoc test.

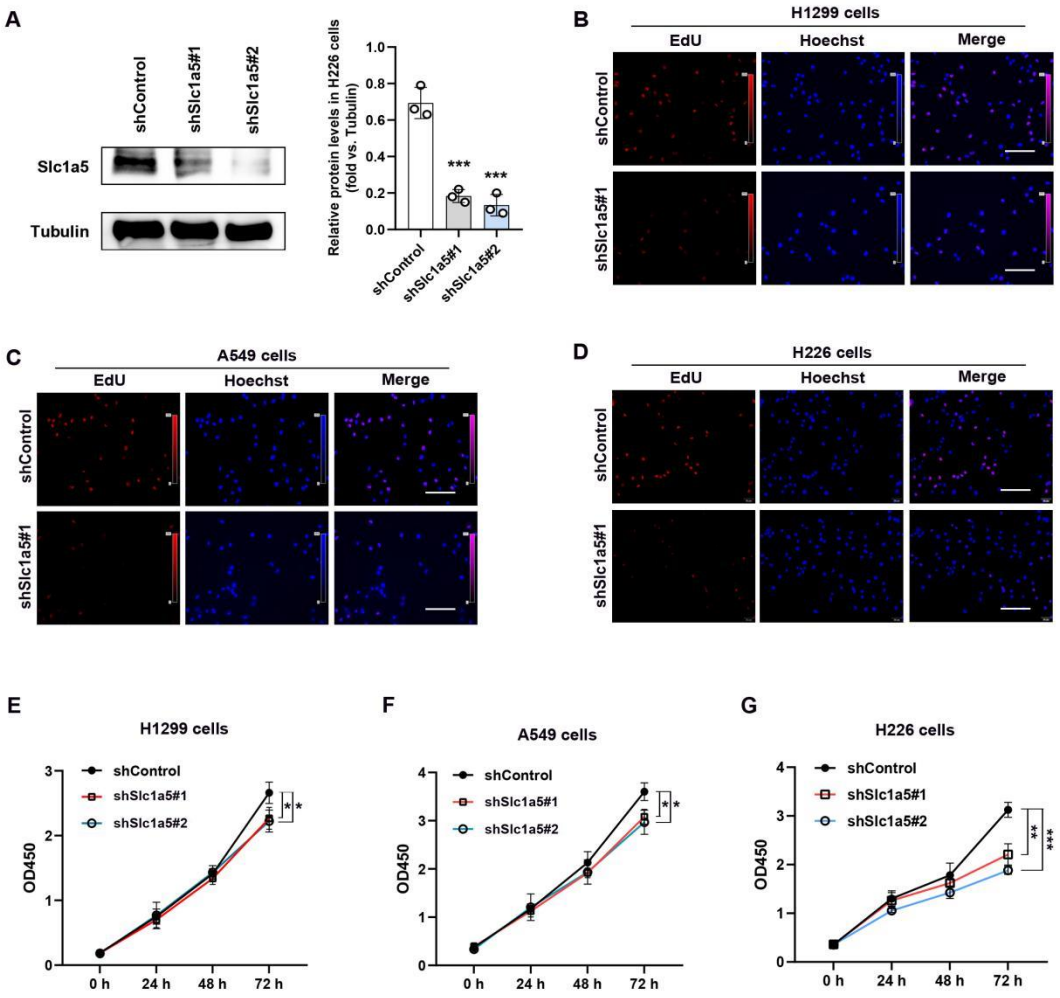

Figure S10. Knockdown of SLC1A5 inhibits the proliferation of H1299, A549 and H226 cells.

(A) Knockdown of SLC1A5 was confirmed at the protein level in H226 cells (n=3).

(B-D) Representative images of EdU and hoechst staining in H1299, A549 and H226 cells, bar=50 μm.

(E-G) CCK-8 assay analysis of cell proliferation in H1299, A549 and H226 cells (n=5). *P ＜0.05, **P＜0.01, ***P＜0.001 vs the shControl group, two-tailed Student's t-test.

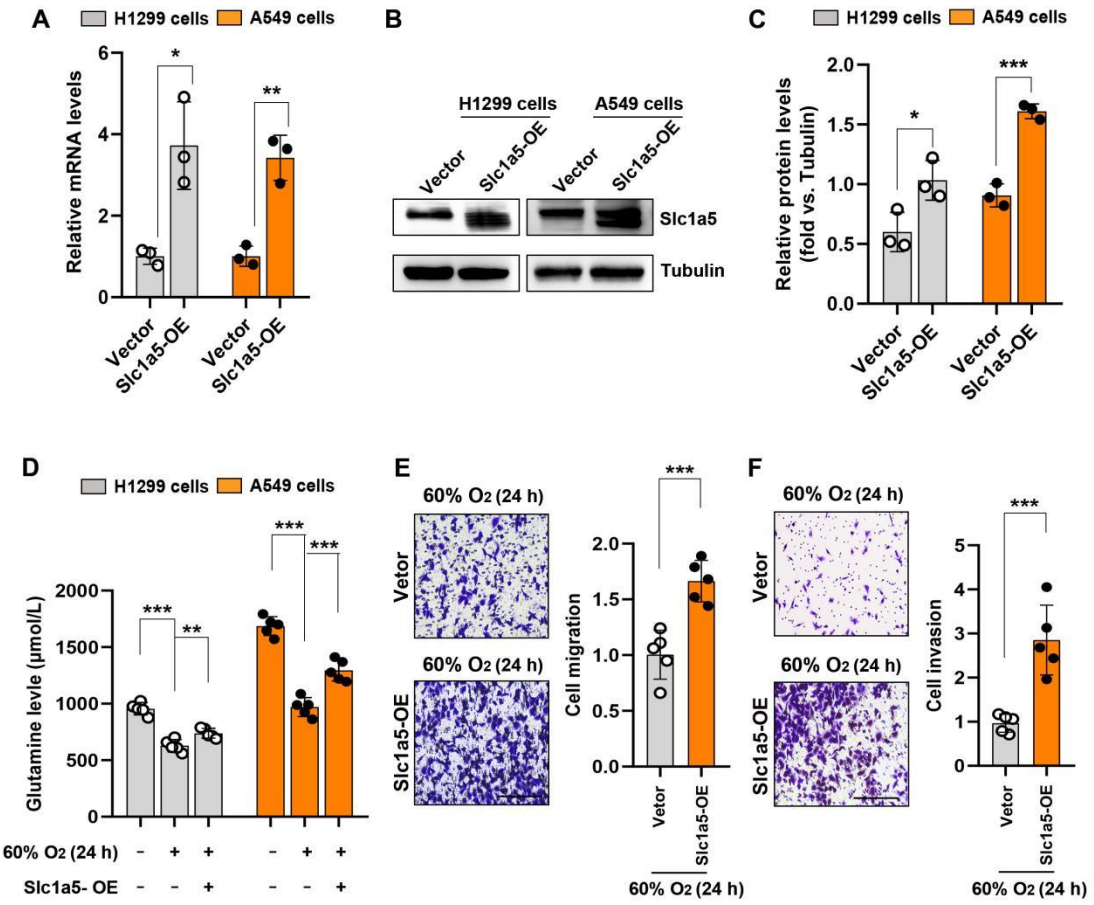

Figure S11. SLC1A5 overexpression increase the intracellular glutamine and cell invasiveness in lung cancer cells with hyperoxia treatment.

(A-C) The gene transfection efficiency was detected by PCR and Western blot analysis in H1299 and A549 cells (n=3).

(D) The levels of glutamine in H1299 and A549 cells (n=5).

(E, F) Effect of SLC1A5 overexpression on the migration and invasion of 60% O_2 (24 h) treated H1299 cells, bar=50 μm.

*P＜0.05, **P＜0.01, ***P＜0.001 vs the indicated group, two-tailed Student's t-test.

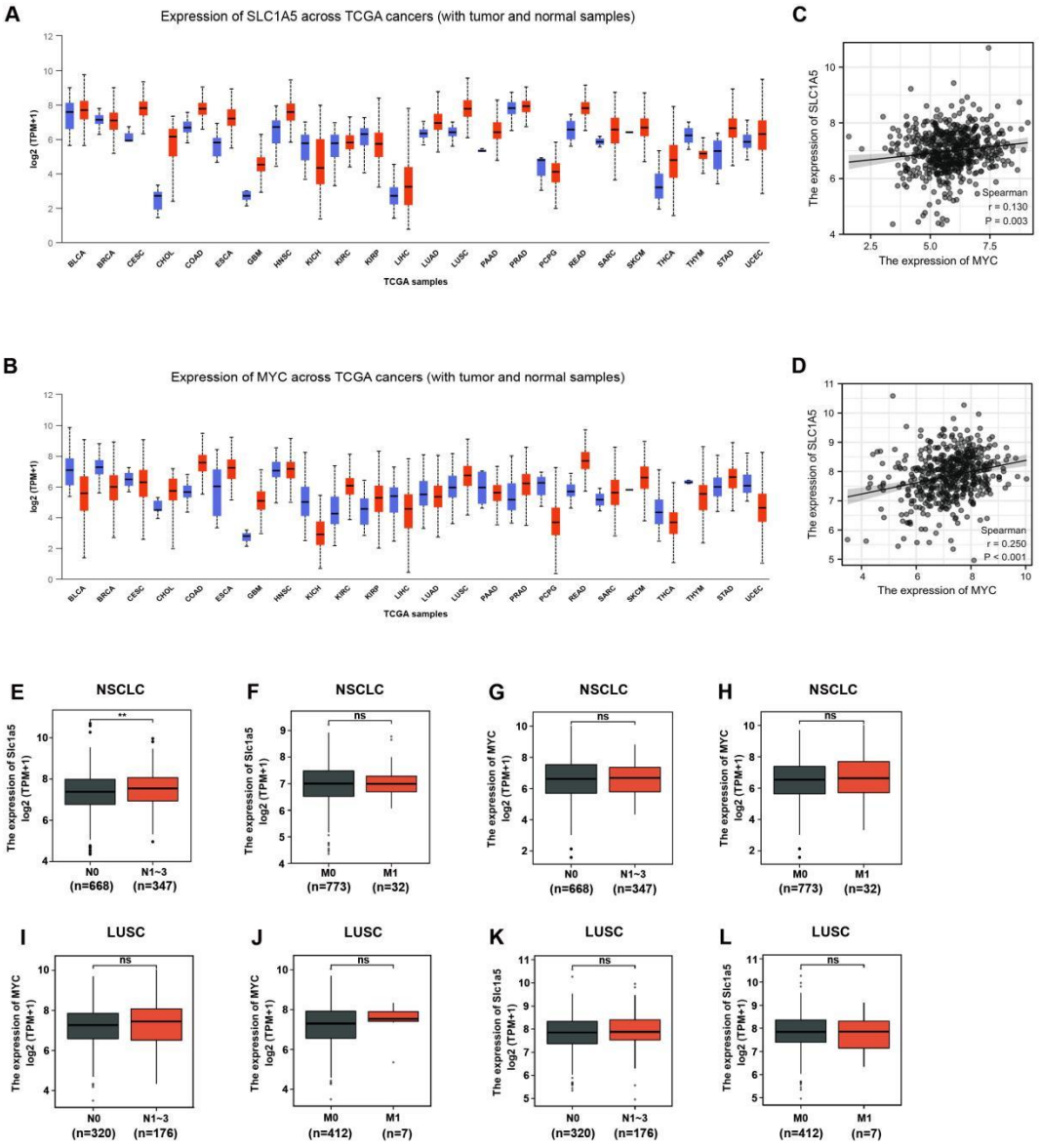

Figure S12. The expression levels of SLC1A5 and MYC are closely related to the clinical characteristics of patients with NSCLC.

(A, B) The expressions of MYC and SLC1A5 in NSCLC tissues and normal tissues was analyzed according to TCGA database.

(C) Correlation between mRNA levels of SLC1A5 versus MYC in LUAD tissues according to TCGA database, r=0.130, *P*=0.003.

(D) Correlation between mRNA levels of SLC1A5 versus MYC in LUSC tissues according to TCGA database, r=0.250, *P*＜0.001.

(E, F) Slc1a5 is increased in NSCLC patients with lymph node metastasis.

(G, H) There was no significant difference in MYC expressions between NSCLC patients with or without metastasis.

(I-L) There was no significant difference in MYC and SLC1A5 expressions between LUSC patients with or without metastasis.

**$P<0.01$, NS, $P>0.05$ vs the N0 or M0 group, two-tailed Student's t-test.